Reply to the comments from Anonymous Referee #2

We deeply appreciate Anonymous Referee #2 for the thorough review of our manuscript. Our manuscript has been revised according to the comments and our responses to the comments are as follows. For clarity, the comments are reproduced in blue, authors' responses are in black and changes in the manuscript are in red color text.

Sea spray aerosol (SSA) formation is an important pathway for the transfer of marine substances to the atmosphere. This study investigates how phytoplankton blooms promote the sea-to-air transfer of dissolved organic carbon (DOC) through SSA formation. Natural seawater was incubated outdoors to induce phytoplankton blooms, and a laboratory waterfall-type SSA simulation tank was used to reproduce the sea—air exchange process. The DOC enrichment in SSA can increase by 10–30 times during phytoplankton blooms, mainly driven by protein-like components (PRLIS), with a secondary contribution from polysaccharides modified by heterotrophic bacteria. The study is well designed and methodologically sound, covering the continuous chain from seawater to the sea surface microlayer and SSA, and it provides scientifically meaningful insights. The following suggestions are provided to the authors for further revision before the final publication.

The continuous plunging waterfall mode was adopted to improve SSA sampling efficiency; however, this configuration may not accurately reproduce the bubble dynamics and turbulence of real oceanic wave-breaking. Please discuss the representativeness and possible implications of this setup.

Author Reply

Plunging waterfall type has been proven as an efficient laboratory simulation method to generate sea spray aerosols (Stokes et al., 2013), and has been used widely in many research studies (Callaghan et al., 2014; Van Acker et al., 2021; Harb and Foroutan, 2022; Jayarathne et al., 2022). Collins et al. conducted a detailed comparison between intermittent and continuous plunging waterfall systems, focusing on differences in sea spray aerosol particle size distribution and organic enrichment (Collins et al., 2014). The main difference between intermittent and continuous modes

lies in how surface foam behavior affects the formation of sea spray aerosol. In intermittent operation, surface foam breaks and dissipates during operational gaps, whereas in continuous operation, foam gradually dissipates as it moves away from the impact point. At lower dissolved organic carbon concentrations (\approx 85 μ M), SSA produced by both methods shows minimal differences, while the differences become more important at higher DOC concentrations (\approx 400 μ M). However, compared to other laboratory SSA production methods (wave breaking and sintered filter glass), the differences between intermittent and continuous plunging waterfalls are relatively minor (Collins et al., 2014). During the phytoplankton bloom period, the use of a continuous plunging waterfall would help reduce our sampling time.

In the revised manuscript, we briefly discuss this configuration.

Page 3, lines 90-94

These two types of plunging waterfalls differ mainly in the behavior of surface bubbles as they rupture and dissipate: in intermittent waterfalls, surface bubbles breaks and dissipates during operational gaps, whereas in continuous waterfalls, surface bubbles gradually dissipates as it moves away from the impact point (Collins et al., 2014).

The enrichment factor (EF) is normalized to Na⁺, assuming its concentration remains constant. However, Na⁺ levels may vary with particle size and humidity. The authors should clarify the measurement range, precision, and variability of Na⁺ and discuss how potential deviations from this assumption could affect the calculated EF values.

Author Reply

The size of SSA is related to relative humidity (RH) as it equilibrates either by absorbing or evaporating water. At different RH, the empirical relationship among the sizes of SSA is: Dp (at 100%RH) ≈ 2 Dp (at 80% RH) ≈ 4 Dp (below 50% RH) (Veron, 2015). In other words, when RH falls below 50%, it is generally considered that water within the SSA has evaporated completely, and the diameter is no longer affected by the water content. In order to exclude the influence of RH on SSA's size, we employed a drying tube to dehumidify the airflow carrying the SSA. After drying, the airflow's

RH was kept below 30%, ensuring that the nascent SSA underwent a phase transition from liquid to solid.

Dried SSA particles were collected by a low-pressure cascade impactor (DLPI+, Dekati Ltd., Finland) and classified into submicron and supermicron SSA. Submicron SSA and supermicron SSA were extracted using 10 mL Milli-Q water. In order to quantify the Na⁺ concentrations, a seven-point calibration curve of 0.1 to 10 μg mL⁻¹ range was created. Samples of seawater and sea surface microlayer were diluted 5,000-fold, and extracts of submicron SSA and supermicron SSA were diluted 5-fold, making the Na⁺ concentrations fall within the range of the calibration curve. The relative standard deviation of Na⁺ concentration after repeated measurements was controlled within 6.2%.

We have added the necessary information in the revised manuscript.

Page 3, lines 94-98

Nascent SSA was transported with purified air (Zero Air Supply, Model 111, Thermo Scientific), and the airflow was dried to a relative humidity below 30% (Monotube Dryer, MD700-12F-3, Perma Pure, USA) before collection and measurement. At this relative humidity, nascent SSA can be completely dried into solid particles.

Additionally, the information regarding the sample dilution, the measurement range of Na⁺ concentration, and the relative standard deviation ranges for multiple measurements has been updated.

Page 5, lines 131-134

Sodium ions (Na⁺) concentrations were measured using an ion chromatograph (Dionex ICS-600, Thermo Fisher Scientific, USA). The seawater and SML samples were diluted 5,000-fold, while the submicron and supermicron SSA extracts were diluted 5-fold, ensuring that their Na⁺ concentrations fall within the 0.1 to 10 μg mL⁻¹ range of a seven-point calibration curve for quantification. Repeated measurements confirmed that the relative standard deviation of the Na⁺ peak area remained within 6.2%.

In the original manuscript, the enrichment factors for organic matter were calculated using the average of multiple measurements. In this revision, we apply uncertainty propagation formulas to incorporate measurement uncertainties into the enrichment factor results. The formulas for calculating the DOC enrichment factor and relative standard deviation (RSD) are as follows:

$$EF = \frac{\left(\mathrm{DOC}\right)_{SSA \text{ or } SML}/\left(\mathrm{Na}^{+}\right)_{SSA \text{ or } SML}}{\left(\mathrm{DOC}\right)_{SW}/\left(\mathrm{Na}^{+}\right)_{SW}}$$

$$RSD_{enrichment \text{ factor}} = \sqrt{\left(RSD_{DOC|SSA \text{ or } SML}\right)^{2} + \left(RSD_{Na}^{+}|SSA \text{ or } SML}\right)^{2} + \left(RSD_{DOC|SW}\right)^{2} + \left(RSD_{Na}^{+}|SW\right)^{2}}$$

In the revised manuscript, we have added explanations regarding the propagation of measurement uncertainty to the enrichment factor calculations and presented the specific settlement results in Figure 3.

Page 5, lines 139-140

Using the uncertainty transfer formula to propagate the uncertainties from multiple measurements results into the calculation of the enrichment factor.

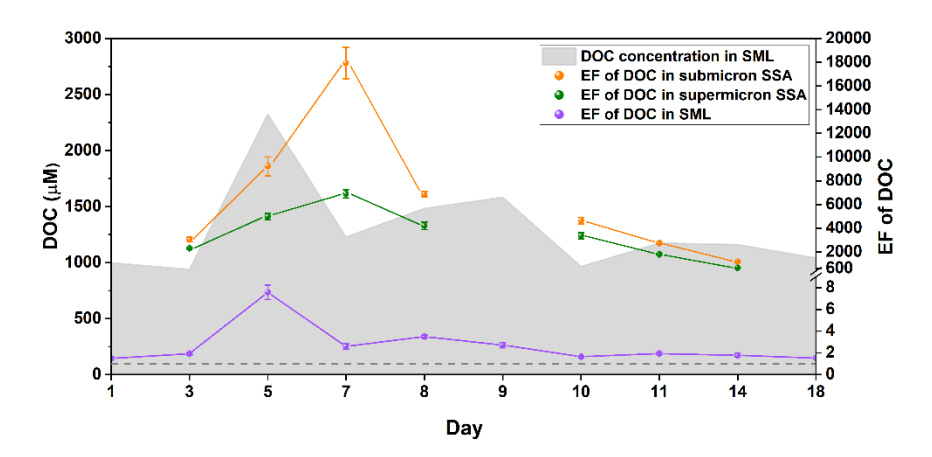


Figure 3. Time series of DOC enrichment during the phytoplankton bloom. Enrichment factors of DOC relative to Na⁺ in the SML (purple), submicron SSA (orange) and supermicron SSA (green). The gray background is the concentration of DOC in the SML. Error bars represent the standard deviation of the EF, derived from the standard deviation of Na⁺ concentration and DOC concentration obtained through multiple measurements.

The fluorescence intensities used in the EEM-PARAFAC analysis may be influenced by matrix effects such as salinity, pH, and the polarity of DOM. These factors can alter fluorescence yield and spectral properties, potentially leading to biases when comparing different sample types (e.g., seawater or SSA extracts). Please include some discussions on how these matrix effects were considered or minimized, and whether they may influence the comparability of EEM results.

Author Reply

Regarding the potential influence of matrix effects—such as salinity, pH, and the polarity of DOM—on fluorescence intensity, these factors could indeed introduce bias between different samples (e.g., seawater versus SSA extracts), which may in turn affect the results of the EEM-PARAFAC analysis.

Changes in pH can alter the ionization state of certain fluorescent compounds, thereby affecting their fluorescence yield (Timko et al., 2015). Seawater and seawater surface microlayer samples used for EEM detection should have a pH of approximately 8.2. In contrast, extracts of submicron and supermicron SSA (extracted with 10 mL of Milli-Q water) contained very low amounts of SSA, leading to pH values close to 7 for these samples.

Salinity variations can influence the aggregation state of fluorescent molecules, thereby altering their fluorescence emission characteristics (Kholodov et al., 2024). While some studies have reported significant enrichment of divalent cations in sea surface microlayer compared to seawater (Salter et al., 2016; Schill et al., 2018), it is important to note that sodium chloride is the main contributor to seawater salinity, with divalent cations contributing relatively little. Therefore, it can be assumed that the salinity of seawater samples and that of SML samples used for EEM fluorescence detection should be quite similar. In contrast, the salinities of submicron and supermicron SSA samples' extracts are both close to and significantly lower than that of seawater.

The matrix effect can potentially influence the absolute intensity of EEM across different samples, particularly due to salinity differences between seawater-type samples (seawater and seawater micro-surface layer) and SSA-type samples

(submicron and supermicron SSA). As a result, the comparability of EEM's absolute intensities between these two categories requires careful verification. Therefore, in the manuscript, our discussion of EEM's absolute intensity in Figure 5(b) is limited to comparisons within each category—either between seawater and sea surface microlayer, or between submicron and supermicron SSA.

When performing EEM-PARAFAC analysis, we accounted for matrix effects and variations in DOC concentrations between seawater and SSA samples. Following the methodology outlined by Murphy et al. (Murphy et al., 2013), we normalized the EEM for each sample to its total signal using the signal normalization module within the drEEM toolbox. This normalization ensures that each sample's EEM contributes equally during the PARAFAC analysis, enabling the model to focus on chemical variations between samples rather than the overall signal magnitude. Additionally, this approach enhances the detection of minor peaks. After model validation, normalization can be cancelled by multiplying the fractions by each sample's total signal intensity.

A discussion on matrix effects, emphasizing their potential impact on fluorescence spectra and acknowledging that these variability sources were considered during data analysis was updated in the revised manuscript

Page 5, lines 144-154

The excitation-emission matrix (EEM) of DOC was obtained using a fluorescence and absorbance spectrometer (DuettaTM, Horiba Scientific, Japan). The excitation wavelength of EEM was in the range of 250-620 nm, the emission wavelength was in the range of 250-700 nm, the scanning intervals were set to 5 nm and 2 nm, respectively, and the slit width was fixed at 5 nm. The EEM results for all samples were normalized to Raman units (R. U.) by the Raman peak of water (Ex=350 nm) after subtracting the background signal obtained from Milli-Q water (Chen et al., 2023). EEM data analysis using parallel factor analysis (PARAFAC) with non-negativity constraints were performed with the DOMFlour toolbox by MATLAB R2020a (Stedmon and Bro, 2008). It is important to consider the matrix effects resulting from differences in pH and salinity between seawater samples (seawater and sea surface microlayer) and SSA samples (submicron and supermicron SSA extracts), as well as potential deviations

from the variability assumptions of the PARAFAC model due to variations in DOC concentrations across the samples. Therefore, we followed the method outlined by Murphy et al. to normalize each sample's EEMs based on their total signal intensity (Murphy et al., 2013). After validating the PARAFAC model through split-half verification and random initialization analysis, the normalization was cancelled by multiplying the fractions by each sample's total signal intensity.

The method recovery, reproducibility, and the detection limit of organic species are suggested to be provided in the method.

Author Reply

We have added this information to the Methods section of the manuscript:

(1) We provided additional details on the dilution factor for the samples, the concentration range of the standard curve, and the relative standard deviation of repeated measurements when measuring Na⁺ concentration using ion chromatography.

Page 5, lines 131-134

Sodium ions (Na⁺) concentrations were measured using an ion chromatograph (Dionex ICS-600, Thermo Fisher Scientific, USA). The seawater and SML samples were diluted 5,000-fold, while the submicron and supermicron SSA extracts were diluted 5-fold, ensuring that their Na⁺ concentrations fall within the 0.1 to 10 µg mL⁻¹ range of a seven-point calibration curve for quantification. Repeated measurements confirmed that the relative standard deviation of the Na⁺ peak area remained within 5.2%.

(2) The number of repetitions for the surface tension measurements, previously described in the caption of Figure 2, has been added to the Methods section.

Page 5, lines 135-136

The surface tension of filtered seawater and SML samples was measured by the platinum plate method using a surface tension meter (Powereach, JB99B, China). Each measurement was repeated three times, and the average value was taken.

(3) In the EEM-PARAFAC method, we have clarified how matrix effects are accounted for during data processing and how variations in dissolved organic carbon concentrations across different samples are addressed.

Page 5, lines 146-154

EEM data analysis using parallel factor analysis (PARAFAC) with non-negativity constraints were performed with the DOMFlour toolbox by MATLAB R2020a (Stedmon and Bro, 2008). It is important to consider the matrix effects resulting from differences in pH and salinity between seawater samples (seawater and sea surface microlayer) and SSA samples (submicron and supermicron SSA extracts), as well as potential deviations from the variability assumptions of the PARAFAC model due to variations in DOC concentrations across the samples. Therefore, we followed the method outlined by Murphy et al. (Murphy et al., 2013) to normalize each sample's EEMs based on their total signal intensity. After validating the PARAFAC model through split-half verification and random initialization analysis, the normalization was cancelled by multiplying the fractions by each sample's total signal intensity.

(4) In Section 2.3.5, we supplemented the average recovery rate for carbohydrate detection.

Page 6, lines 168-170

The quantification was performed using seven-point standardized calibration curves with concentrations ranging from 10 nM to 10 μ M. According a previous assessment, the desalting dialysis step retains over 90% of high-molecular-weight DOC (Engel and Händel, 2011); after acidification and hydrolysis, the average recovery rate for most saccharides ranges from 81% to 107%.

Please specify in the abstract whether the reported "10-fold to 30-fold enrichment" of DOC refers to SW or to the SML.

Author Reply

We have included the specification in the revised abstract.

Page 1, lines 17-19

In this study, we observed that the phytoplankton bloom can promote DOC

enrichment in SSA by 10- to 30-fold compared to seawater and investigated the mechanism of DOC sea-to-air transfer using various characterization tools.

Ensure consistent color scales in Figure 5 EEM panels to enable visual comparison.

Author Reply

After careful consideration of the Referee's suggestion and reviewing relevant literature, we have decided to retain the different color scales. The specific reasons are as follows:

Figure 5a shows the three types of fluorescent chromophores, which coexist in seawater, the SML, submicron SSA, and supermicron SSA, identified through the EEM-PARAFAC method. Since the identification of fluorescent chromophores relies primarily on the excitation and emission wavelengths corresponding to the peak fluorescence signals, selecting an appropriate color scale is crucial for accurately depicting the positions of these peaks.

The fluctuations in both absolute and relative fluorescence intensities of these three fluorescent substances during different phytoplankton blooms are shown in Figures 5b and 5c, allowing for visual comparison.

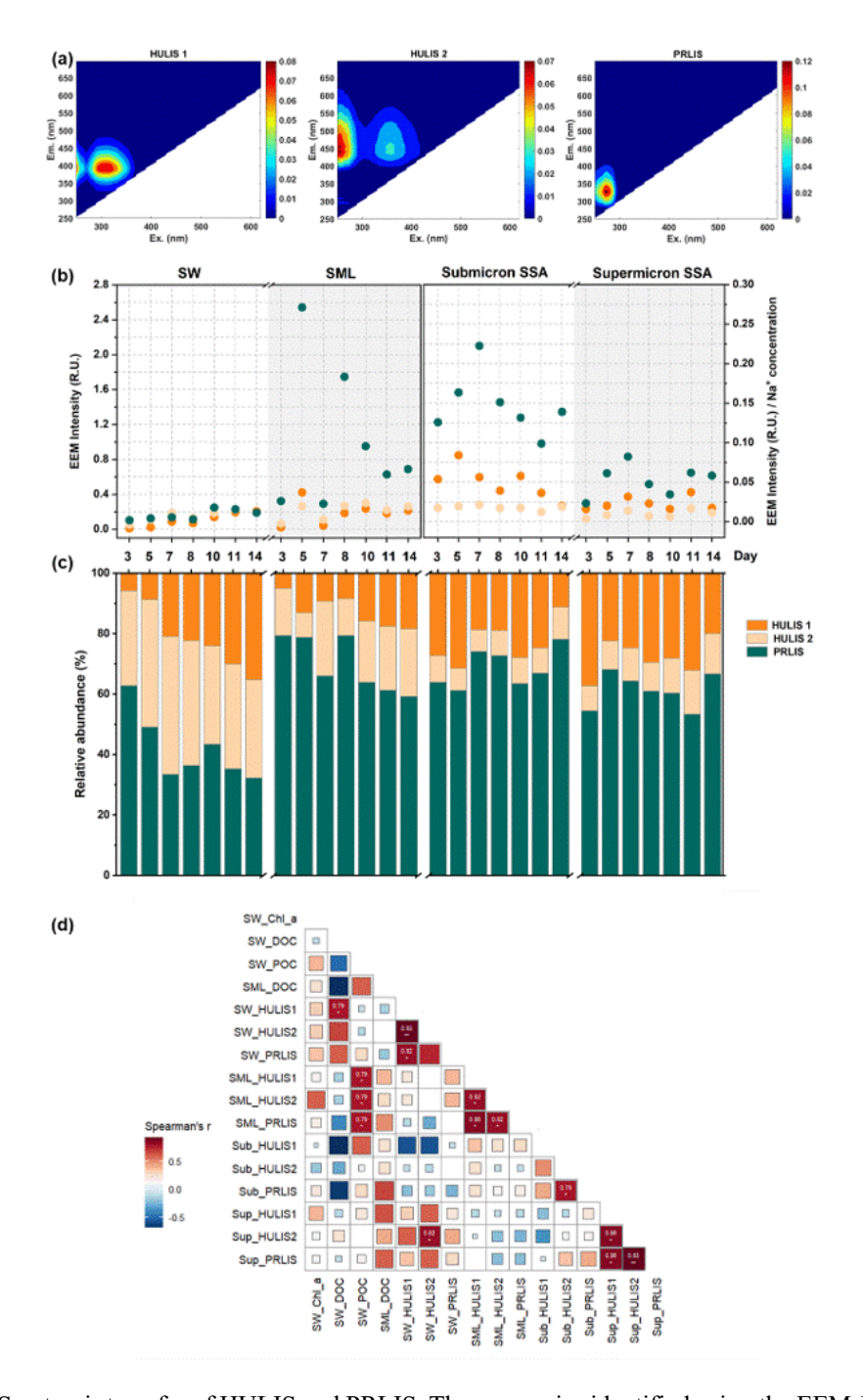


Figure 5. Sea-to-air transfer of HULIS and PRLIS. Three organics identified using the EEM-PARAFAC method: (a) HULIS 1, HULIS 2, and PRLIS. (b) EEM intensities of the three organics in different samples with respect to time. Note that in order to exclude the effect of SSA collection mass on EEM intensity, EEM intensities of SSA samples were normalized with their Na⁺ concentrations. (c) Relative abundance of EEM intensities of the three organics in different samples with respect to time. (d) Spearman's correlation between Chl-a, DOC and POC concentrations in seawater, POC concentration in the SML and EEM intensities of three fluorescent substances.

Add standard deviation or error bars for EF values to better exhibit measurement uncertainty.

Author Reply

Measurement uncertainties into the enrichment factor results were obtained by applying the uncertainty propagation formulas. These formulas for calculating the DOC enrichment factor and relative standard deviation (RSD) are as follows:

$$EF = \frac{\left(DOC\right)_{SSA \text{ or } SML}/\left(Na^{^{+}}\right)_{SSA \text{ or } SML}}{\left(DOC\right)_{SW}/\left(Na^{^{+}}\right)_{SW}}$$

$$RSD_{enrichment \text{ factor}} = \sqrt{\left(RSD_{DOC|SSA \text{ or } SML}\right)^{2} + \left(RSD_{Na^{^{+}}|SSA \text{ or } SML}\right)^{2} + \left(RSD_{DOC|SW}\right)^{2} + \left(RSD_{Na^{^{+}}|SW}\right)^{2}}$$
 We have added error bars to Figure 3 and updated the figure.

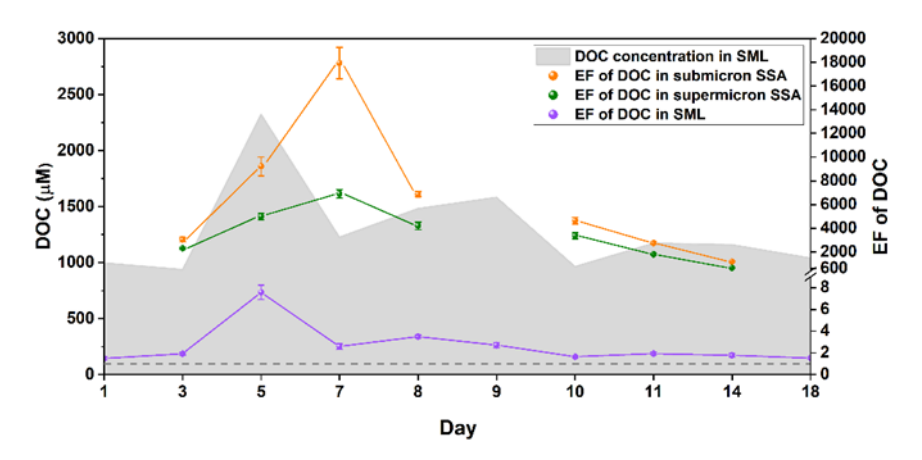


Figure 3. Time series of DOC enrichment during the phytoplankton bloom. Enrichment factors of DOC relative to Na⁺ in the SML (purple), submicron SSA (orange) and supermicron SSA (green). The gray background is the concentration of DOC in the SML. Error bars represent the standard deviation of the EF, derived from the standard deviation of Na⁺ concentration and DOC concentration obtained through multiple measurements.

References

Callaghan, A. H., Stokes, M. D., and Deane, G. B.: The effect of water temperature on air entrainment, bubble plumes, and surface foam in a laboratory breaking-wave analog, J. Geophys. Res. Oceans, 119, 7463-7482, 2014.

Chen, H., Yan, C., Fu, Q., Wang, X., Tang, J., Jiang, B., Sun, H., Luan, T., Yang, Q., Zhao, Q., Li, J., Zhang, G., Zheng, M., Zhou, X., Chen, B., Du, L., Zhou, R., Zhou, T., and Xue, L.: Optical properties and molecular composition of wintertime atmospheric water-soluble organic carbon in different coastal cities of eastern China, Sci. Total Environ., 892, 164702,

- https://doi.org/10.1016/j.scitotenv.2023.164702, 2023.
- Collins, D. B., Zhao, D. F., Ruppel, M. J., Laskina, O., Grandquist, J. R., Modini, R. L., Stokes, M. D., Russell, L. M., Bertram, T. H., Grassian, V. H., Deane, G. B., and Prather, K. A.: Direct aerosol chemical composition measurements to evaluate the physicochemical differences between controlled sea spray aerosol generation schemes, Atmos. Meas. Tech., 7, 3667-3683, 2014.
- Engel, A. and Händel, N.: A novel protocol for determining the concentration and composition of sugars in particulate and in high molecular weight dissolved organic matter (HMW-DOM) in seawater, Mar. Chem., 127, 180-191, https://doi.org/10.1016/j.marchem.2011.09.004, 2011.
- Harb, C. and Foroutan, H.: Experimental development of a lake spray source function and its model implementation for Great Lakes surface emissions, Atmos. Chem. Phys., 22, 11759-11779, https://doi.org/10.5194/acp-22-11759-2022, 2022.
- Jayarathne, T., Gamage, D. K., Prather, K. A., and Stone, E. A.: Enrichment of saccharides at the airwater interface: a quantitative comparison of sea surface microlayer and foam, Environ. Chem., 19, 506-516, https://doi.org/10.1071/EN22094, 2022.
- Kholodov, V. A., Danchenko, N. N., Ziganshina, A. R., Yaroslavtseva, N. V., and Semiletov, I. P.: Direct Salinity Effect on Absorbance and Fluorescence of Chernozem Water-Extractable Organic Matter, Aquatic Geochemistry, 30, 31-48, 10.1007/s10498-024-09423-w, 2024.
- Murphy, K., Stedmon, C., Graeber, D., and Bro, R.: Fluorescence spectroscopy and multi-way techniques. PARAFAC, Anal. Methods, 5, 6541–6882, 10.1039/c3ay41160e, 2013.
- Salter, M. E., Hamacher-Barth, E., Leck, C., Werner, J., Johnson, C. M., Riipinen, I., Nilsson, E. D., and Zieger, P.: Calcium enrichment in sea spray aerosol particles, Geophys. Res. Lett., 43, 8277-8285, 2016.
- Schill, S. R., Burrows, S. M., Hasenecz, E. S., Stone, E. A., and Bertram, T. H.: The Impact of Divalent Cations on the Enrichment of Soluble Saccharides in Primary Sea Spray Aerosol, Atmosphere, 9, 476, 2018.
- Stedmon, C. A. and Bro, R.: Characterizing dissolved organic matter fluorescence with parallel factor analysis: a tutorial, Limnol. Oceanogr. Meth., 6, 572-579, https://doi.org/10.4319/lom.2008.6.572, 2008.
- Stokes, M. D., Deane, G. B., Prather, K., Bertram, T. H., Ruppel, M. J., Ryder, O. S., Brady, J. M., and Zhao, D.: A Marine Aerosol Reference Tank system as a breaking wave analogue for the production of foam and sea-spray aerosols, Atmos. Meas. Tech., 6, 1085-1094, https://doi.org/10.5194/amt-7-3667-2014, 2013.
- Timko, S. A., Gonsior, M., and Cooper, W. J.: Influence of pH on fluorescent dissolved organic matter photo-degradation, Water Res., 85, 266-274, https://doi.org/10.1016/j.watres.2015.08.047, 2015.
- Van Acker, E., Huysman, S., De Rijcke, M., Asselman, J., De Schamphelaere, K. A. C., Vanhaecke, L., and Janssen, C. R.: Phycotoxin-Enriched Sea Spray Aerosols: Methods, Mechanisms, and Human Exposure, Environ. Sci. Technol., 55, 6184-6196, 10.1021/acs.est.1c00995, 2021.
- Veron, F.: Ocean Spray, Annu. Rev. Fluid Mech., 47, 507-538, https://doi.org/10.1146/annurev-fluid-010814-014651, 2015.